Film coating by directional droplet spreading on fibers

Tak Shing Chan,[1,*] Carmen L. Lee,[2,*] Christian Pedersen,[1] Kari Dalnoki-Veress,[2,3] and Andreas Carlson[1,†]

[1]*Department of Mathematics, Mechanics Division, University of Oslo, N-0851 Oslo, Norway*
[2]*Department of Physics and Astronomy, McMaster University, 1280 Main Street West, Hamilton, Ontario, Canada L8S 4M1*
[3]*UMR CNRS Gulliver 7083, ESPCI Paris, PSL Research University, 75005 Paris, France*

(Received 10 August 2020; accepted 15 December 2020; published 20 January 2021)

Plants and insects use slender conical structures to transport and collect small droplets, which are propelled along the conical structures due to capillary action. These droplets can deposit a fluid film during their motion, but despite its importance to many biological systems and industrial applications, the properties of the deposited film are unknown. We characterize the film deposition by developing an asymptotic analysis together with experimental measurements and numerical simulations based on the lubrication equation. We show that the deposited film thickness depends significantly on both the fiber radius and the droplet size, highlighting that the coating is affected by finite-size effects relevant to film deposition on fibers of any slender geometry. We demonstrate that by changing the droplet size, while the mean fiber radius and the capillary number are fixed, the thickness of the deposited film can change by an order of magnitude or more. We show that self-propelled droplets have significant potential to create passively coated structures.

DOI: 10.1103/PhysRevFluids.6.014004

I. INTRODUCTION

Droplets on slender conical substrates will self-propel due to capillary action [1–10] provided the droplets are smaller than the capillary length. This principle is used by insects [11,12] and plants [13–20] for droplet collection. Several studies have focused on mimicking structures found in nature to control liquid movement [21–27]. Recent work [13] has shown that the conically shaped trichomes on the underside of the lid of the *Sarracenia*, a pitcher plant, can transport droplets with a velocity several orders of magnitude larger than that found in other plants. Enhanced water transport is the result of surface lubrication of the trichome. The first droplet that slowly spreads across the trichome deposits a microscopic liquid film, and the following droplets slide along the lubricating film on the trichome. From a technological point of view, understanding the principles of film deposition by capillary-driven motion of droplets can provide pathways for relubrication of slippery liquid infused porous surfaces with conical shapes [6,28] as well as the development of other multifunctional materials. This lubricating film-coating principle has a fundamental role in biological phenomena and has untapped potential as a droplet-driven coating technique, yet the properties of the liquid film are unknown. We study here how droplets deposit lubricating films as they move along slender structures.

*These authors contributed equally to this work.
†acarlson@math.uio.no

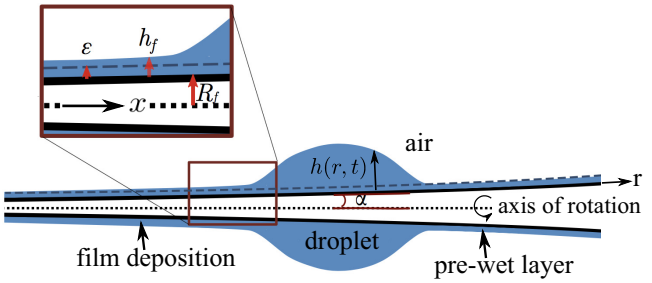

FIG. 1. (a) A sketch of a droplet on a conical fiber with a local cone angle α. Inset: zoom into the region connecting the deposited film of thickness h_f and the receding edge of the droplet at the fiber radius R_f. The fiber is prewet with a layer of the same fluid of thickness ϵ.

Coating a solid substrate with a lubricating liquid film as a way to reduce friction between substrates has been known since ancient Egypt [29]. The broad relevance of coating processes have made them widely studied, with great advances in understanding their underlying physical principles [30–34]. Dip-coating is today one of the most widespread coating techniques [35], where the solid moves with a velocity U relative to the liquid bath. The foundational work of Landau-Levich-Derjaguin (LLD) [36,37] has paved the way for a fundamental understanding of film deposition on solid substrates during wetting. By considering the viscous capillary flow of a liquid with a viscosity μ and a surface tension γ, LLD predicted that the deposited film thickness h_f, normalized by the characteristic length of the system L, is given by $h_f/L \sim \mathrm{Ca}^{2/3}$ [36,37], where the Capillary number $\mathrm{Ca} \equiv \mu U/\gamma$ is the ratio of the viscous and surface tension forces. The LLD theory was developed for $\mathrm{Ca} \ll 1$ and when inertia can be neglected. It is a generic scaling and has proven to be an accurate description of a wide range of coating phenomena, i.e., dip coating of plates [38], cylinders [31,39,40], and Bretherton bubbles [41]. However, a droplet depositing a film on a cylinder has a fundamental difference from film deposition from a liquid reservoir; the droplet size introduces another length scale to the system. The fiber geometry and droplet size are tuneable parameters to control the coating process [1,2].

II. THEORY AND EXPERIMENT

In the system studied here, a droplet deposits a film as it migrates toward the thicker part of a prewet conical fiber, driven by the curvature gradient, as shown schematically in Fig. 1. We investigate the system by combining asymptotic analysis, experiments, and numerical simulations. The assumptions made are that there is viscous flow driven by capillarity ($\mathrm{Ca} \ll 1$). Furthermore, we neglect gravitational effects because the drop size is much smaller than the capillary length, as is clear from the Bond number, which represents the balance between gravity and surface tension, $\mathrm{Bo} = \Delta\rho g V^{2/3}/\gamma \ll 1$, where $\Delta\rho$ is the density difference between the liquid and surrounding air, V is the droplet volume, and g is the gravitational acceleration. As will be seen below, these assumptions are verified by our experiments.

A. Asymptotic analysis

We start off by revising the classical LLD theory for the case of a droplet moving on a cylindrical fiber with radius R by matching asymptotically the quasistatic droplet profile on the fiber $h_s(x)$ and the self-similar deposited film profile (for details, see [4]). By matching the profiles, we show that the film thickness h_f scales with Ca as [4]

$$h_f = 1.338\ell \mathrm{Ca}^{2/3}, \tag{1}$$

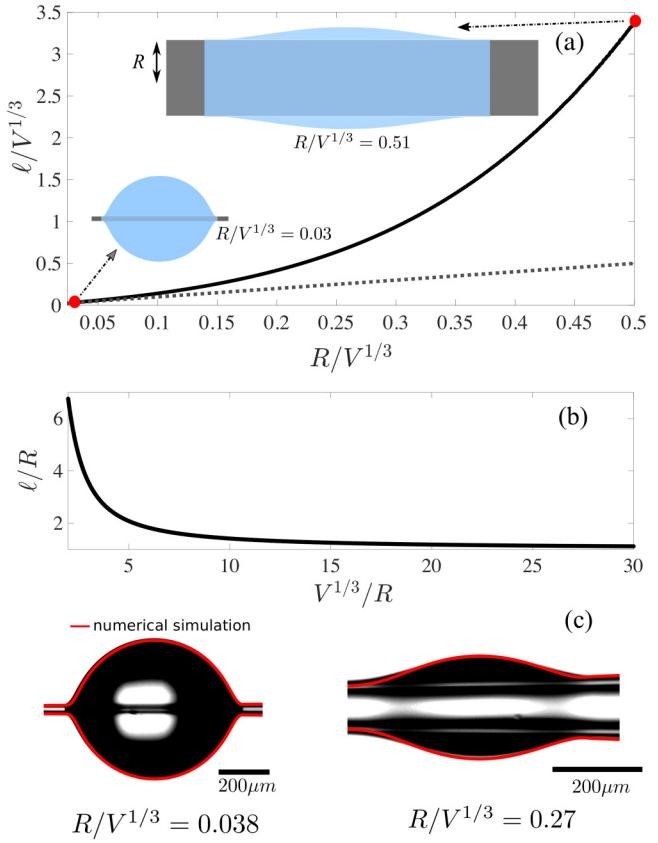

FIG. 2. (a) The dimensionless characteristic length $\ell/V^{1/3}$ as a function of the rescaled radius $R/V^{1/3}$ of a cylindrical fiber (solid line). The dotted line represents the linear relation, i.e., $\ell = R$. Inset: two static droplets of the same volume in contact with a fiber with $R/V^{1/3} = 0.03$ and 0.51 (indicated by the two red dots), which demonstrate different droplet shapes when R varies. The deposited film thickness h_f predicted by our asymptotic analysis scales linearly with ℓ for a given Capillary number Ca (dimensionless droplet velocity); see Eq. (1). From (a) we see that a droplet of a fixed volume coats a thicker film on a thicker fiber. In (b), ℓ rescaled by the fiber radius R is plotted as a function of $V^{1/3}/R$. It shows that for the same fiber radius, a smaller droplet coats a thicker film on the fiber. (c) Sample images of two droplets taken with optical microscopy (top views). Left: $\alpha = 0.43^\circ$ and $R/V^{1/3} = 0.038$, and right: $\alpha = 2.5^\circ$ and $R/V^{1/3} = 0.27$. The numerically calculated profiles from the lubrication theory on a cone [Eq. (2)] are shown in red for matching V, R, and α.

where $\ell \equiv 1/[\partial^2 h_s(x = x_{\rm cl})/\partial x^2]$ is the inverse of the second derivative of the static profile $h_s(x)$ evaluated at the contact line position $x = x_{\rm cl}$, i.e., where the profile $h_s(x)$ meets the solid substrate. A crucial difference from the classical LLD theory is that choosing $\ell = R$ only recovers the correct film thickness in the limit of $R \ll V^{1/3}$. In general, ℓ depends on both the droplet volume V and the fiber radius R, which indicates a finite-size effect. To illustrate this point, we plot $\ell/V^{1/3}$ as a function of $R/V^{1/3}$ in Fig. 2(a). In the limit where $R \ll V^{1/3}$, $\ell = R$, then the film thickness $h_f = 1.338R\,{\rm Ca}^{2/3}$ is independent of the droplet volume. However, when $R/V^{1/3} \gtrsim 0.15$, the droplet size starts to play a significant role in predicting the deposited film thickness that is much larger than if we would naively assume $\ell = R$. Since $\ell/V^{1/3}$ increases with $R/V^{1/3}$ faster than a linear relation, Eq. (1) also implies that a smaller droplet deposits a thicker film for fixed R and Ca. This property is shown in Fig. 2(b), in which ℓ/R decreases with increasing $V^{1/3}/R$. For the directional spreading of droplets

on a conical fiber with a small cone angle α, the influence of α on ℓ only appears as high-order corrections, which are neglected here (see [4] for details). The conical geometry acts as a factor that generates the spontaneous motion of the droplet and plays a role in determining the magnitude of Ca. The theoretical prediction for the film thickness dependence on the droplet size and the fiber radius [see Eq. (1)] can now be compared to experiments and numerical simulations based on the lubrication theory.

B. Experiments

The conical substrates used in the experiments are prepared by pulling standard borosilicate glass capillary tubes in a magnetic micropipette puller (Narishige PN-30). The resulting shape of the capillary tube is a nearly conical fiber with a smoothly varying diameter and gradient, with a smaller cone angle nearing the tip of the fiber. The gradient in the cone angle varies slowly along the fiber, thus on the length scale of the droplet the fibers can be treated as ideal. Droplets of silicone oil with viscosity of $\mu \approx 4.9$ Pa s, and with air-liquid surface tension $\gamma = 22$ mN/m, were deposited at the fiber tip. Silicone oil is ideal because it is totally wetting, chemically stable, nonvolatile, and nonhygroscopic. The fiber is prewet by placing a droplet on the tip of the fiber and allowing it to migrate from one end of the fiber to the other, thereby depositing a film. Prewet film thicknesses were found to range from 0.27 to 13.87 μm, as determined by optical microscopy (OM) using an upright microscope (Olympus BX51) with bottom illumination. OM images of the fiber were taken from above both before and after coating, and they were used to obtain the film thickness. Droplets of volumes V in the range of 0.009–1.99 mm^3, i.e., Bo $\in$ [0.02-0.7], were deposited onto the fiber. Images of the droplet are taken as it migrates along the fiber at a given radius R, and the deposited film is observed as the droplet passes a given location. To ensure the effects of gravity are not affecting the dynamics, a similar experiment was performed in which the entire experimental setup was tilted at different angles to measure if there were any changes in droplet motion in the plane of gravity. There were no discernible differences in droplet motion, and thus the effects of gravity are negligible. The radii of the cone at the measured film thicknesses ranged between 22.26 and 103.92 μm and the deposited film thicknesses were measured in the range of 0.17–19.75 μm.

C. Numerical simulations

To give a mathematical description of the droplet flow on the prewet fiber, we turn to the lubrication approximation for the viscous incompressible flow, when the cone angle $\alpha \ll 1$. The thin-film equation is obtained by reducing the Navier-Stokes equations for flow in films with large lateral dimensions in relation to the thickness [42,43], in combination with mass conservation. A detailed derivation of the lubrication approximation on a conical geometry for $\alpha \ll 1$ is found in [3]. Note that we impose a no-slip condition at the solid substrate and no-shear stress at the free surface. The axisymmetric liquid-air interface profile is given by $h = h(r, t)$, defined as the distance between the interface and the substrate, as a function of the radial distance from the vertex of the cone r and time t. The evolution of the free surface is described by [3,4],

$$\frac{\partial h}{\partial t} + \frac{1}{r\alpha + h}\frac{\partial}{\partial r}\left(M\frac{\partial p}{\partial r}\right) = 0, \tag{2}$$

where the mobility $M = M(h, r, \alpha)$ reads

$$M(h, r, \alpha) = \frac{r^4\alpha^4}{2\mu}\left\{\frac{1}{8}\left[3\left(1 + \frac{h}{r\alpha}\right)^4 - 4\left(1 + \frac{h}{r\alpha}\right)^2 + 1\right] - \frac{1}{2}\left(1 + \frac{h}{r\alpha}\right)^4 \ln\left(1 + \frac{h}{r\alpha}\right)\right\}. \tag{3}$$

The capillary pressure gradient in the liquid generates the flow, and the pressure $p = p(r, t)$ reads

$$p = -\gamma\left\{\frac{\frac{\partial^2 h}{\partial r^2}}{\left[1 + \left(\frac{\partial h}{\partial r}\right)^2\right]^{3/2}} - \frac{1 - \alpha\frac{\partial h}{\partial r}}{(r\alpha + h)\left[1 + \left(\frac{\partial h}{\partial r}\right)^2\right]^{1/2}}\right\}, \tag{4}$$

where the expression is simplified for $\alpha \ll 1$ [3,4]. Equations (2) and (4) are discretized by linear elements and numerically solved with a Newton solver by using the open source finite-element code FEniCS [44]; additional details about the numerical approach are found in [4]. The initial condition is a droplet smoothly connected to a prewet film of thickness ϵ. At the two boundaries ($\delta\Omega$) of the numerical domain, we impose $h(\delta\Omega, t) = \epsilon$ and $p(\delta\Omega, t) = \gamma/R(\delta\Omega)$, where $R(\delta\Omega)$ is the radius of the cone at the boundaries. We note that only the droplet volume V is important, and the initial droplet shape does not affect the results.

III. RESULTS AND DISCUSSION

We start by comparing the droplet spreading dynamics on two cones with $\alpha = 0.43^\circ$ and 2.5°, where the droplet quickly relaxes from its initial condition to its quasistatic shape and then starts to translate to the thicker part of the fiber. When we overlay the experimental measurement with the numerical simulations, as shown in Fig. 2(c), we see that the two results are in close agreement. By zooming into the trailing edge of the droplet, both the experiment and the numerical simulation show the deposition of a film of different thickness from that of the prewet film ϵ.

Next we turn to characterize the thickness of the film during the droplet spreading dynamics on the fiber. To determine the Ca, we extract the droplet velocity U measured at its center of mass. The film is measured on the cone after the droplet has deposited the film, which is stable throughout the observation time in the experiments and the numerical simulations. The Rayleigh-Plateau instability is expected to take place at much longer times as the time scale of the fastest growing mode for a film coated on a cylinder with similar radius is predicted to be more than an order of magnitude longer than both the experimental observation time and the simulation time. Since there is a slight gradient in the cone angle along r in the fiber used in the experiments, we extract the cone angle locally at a given position on the cone with radius $R = R_f$. Here R_f is the cone radius in the receding region, defined based on the droplet profile; see [4]. The deposited film thickness h_f is then a function of α, R_f, V, and ϵ. We combine all the experimental measurements and the numerical predictions of $h_f \in [0.17 - 19.75]$ μm, i.e., for $\alpha \in [0.35 - 2.3]^\circ$, in Fig. 3(a), and they are in good agreement. The film thickness is not uniform along the fiber for a fixed cone angle, but increases with the cone radius R_f. The film thickness h_f increases by roughly one order of magnitude when the cone angle α is varied from 0.35° to 2.3°.

To further compare the theory to the experiments and numerical simulations, we rescale our measurements according to Eq. (1) and also plot the analytical prediction; see Fig. 3(b). Since the motion of the droplet is driven by capillarity, i.e., it is self-propelled, the droplet velocity is a function of the position on the cone. The deposited film thickness h_f rescaled by ℓ obtained from the experiments and the lubrication theory on a cone is shown as a function of Ca in Fig. 3(b). When comparing the results (1) predicted by the asymptotic matching, the experiments, and the numerical simulations, we observe that they are in close agreement, especially for the smallest cone angles. When α increases, there is a slight deviation from $2/3$ scaling observed in the numerical simulations with a slightly larger film thickness than predicted from Eq. (1), likely a consequence of the reduced separation of length scales between the film thickness h_f and the droplet size $V^{1/3}$.

We show that self-propelled droplets have a significant potential to create passively coated structures. By combining an asymptotic analysis, experiments, and numerical simulations of the lubrication equation, we have demonstrated that a droplet that moves on a fiber can deposit a film with a thickness h_f, controlled by the droplet's capillary number and the characteristic length ℓ. The quantity ℓ is a geometric factor that is linear with respect to the fiber radius R when $R/V^{1/3} \ll 1$, i.e., the droplet is much greater in size than the fiber radius. Otherwise, $\ell/V^{1/3}$ increases significantly with $R/V^{1/3}$ when $R/V^{1/3} \gtrsim 0.15$. Our finding has direct implications for control of film deposition during spreading, e.g., if we fix the fiber radius, decreasing the droplet size can increase the thickness of the deposited film by an order of magnitude or more at the same Ca. Coating by droplets introduces novel design features that do not exist in classical coating techniques where the substrate is connected to a liquid reservoir. For a droplet moving on a cylindrical fiber driven

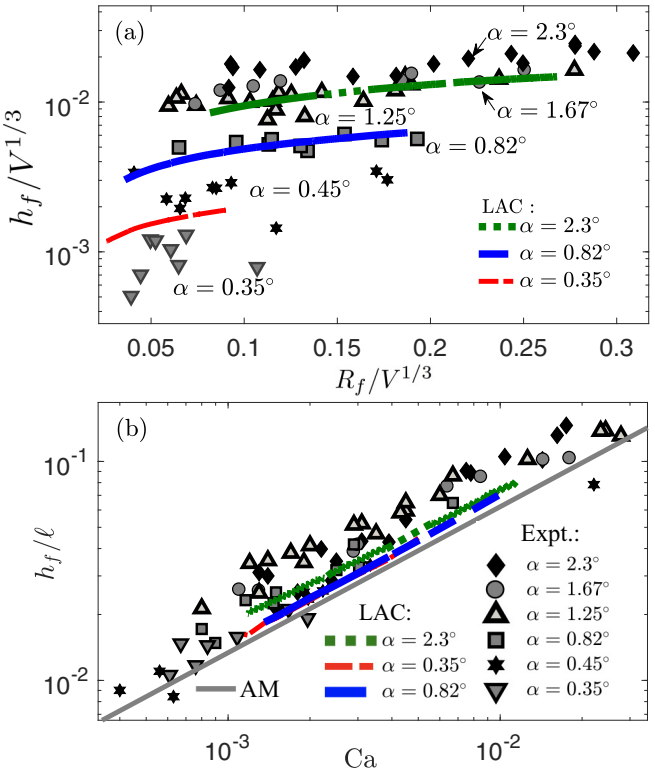

FIG. 3. (a) The deposited film thickness h_f as a function of the cone radius R_f and the cone angle α. Both axes are normalized by $V^{1/3}$. Symbols are experimental data and curves are numerical results from the lubrication theory on a cone (LAC). The prewet layer thickness ϵ in both the experiment and the theory is controlled within a range of 0.27-13.87 μm. (b) The film thickness h_f rescaled by ℓ as a function of the capillary number Ca. The solid line (AM) is the result of asymptotic matching given by Eq. (1).

by external forces, e.g., electric, magnetic, and gravitational, the deposited film thickness follows Eq. (1), whereas Ca depends on the magnitude of the driving force. Our findings are expected to be relevant for any droplet coating application involving a slender geometry, and they may help shed light on why slender conical structures have evolved in a diverse set of biological systems to facilitate efficient droplet transport.

ACKNOWLEDGMENTS

T.S.C. and A.C. gratefully acknowledge financial support from the Research Council of Norway (Project No. 301138) and the UiO:LifeScience initiative at the University of Oslo. C.L.L. and K.D.-V. acknowledge financial support from the Natural Science and Engineering Research Council of Canada.

[1] É. Lorenceau and D. Quéré, Drops on a conical wire, J. Fluid Mech. **510**, 29 (2004).
[2] E. Q. Li and S. T. Thoroddsen, The fastest drop climbing on a wet conical fibre, Phys. Fluids **25**, 052105 (2013).
[3] T. S. Chan, F. Yang, and A. Carlson, Directional spreading of a viscous droplet on a conical fibre, J. Fluid Mech. **894**, A26 (2020).

[4] T. S. Chan, C. Pedersen, J. Koplik, and A. Carlson, Film deposition and dynamics of a self-propelled wetting droplet on a conical fibre, J. Fluid Mech. **907**, A29 (2021).
[5] Y.-E. Liang, H.-K. Tsao, and Y.-J. Sheng, Drops on hydrophilic conical fibers: Gravity effect and coexistent states, Langmuir **31**, 1704 (2015).
[6] J. McCarthy, D. Vella, and A. A. Castrejón-Pita, Dynamics of droplets on cones: Self-propulsion due to curvature gradients, Soft Matter **15**, 9997 (2019).
[7] P. Renvoisé, J. W. M. Bush, M. Prakash, and D. Quéré, Drop propulsion in tapered tubes, Europhys. Lett. **86**, 64003 (2009).
[8] T.-H. Chou, S.-J. Hong, Y.-E. Liang, H.-K. Tsao, and Y.-J. Sheng, Equilibrium phase diagram of drop-on-fiber: Coexistent states and gravity effect, Langmuir **27**, 3685 (2011).
[9] J.-L. Liu, R. Xia, B.-W. Li, and X.-Q. Feng, Directional motion of droplets in a conical tube or on a conical fibre, Chin. Phys. Lett. **24**, 3210 (2007).
[10] X.-F. Wu and Y. A. Dzenis, Droplet on a fiber: Geometrical shape and contact angle, Acta Mech. **185**, 215 (2006).
[11] Y. Zheng, H. Bai, Z. Huang, X. Tian, F.-Q. Nie, Y. Zhao, J. Zhai, and L. Jiang, Directional water collection on wetted spider silk, Nature (London) **463**, 640 (2010).
[12] A. R. Parker and C. R. Lawrence, Water capture by a desert beetle, Nature (London) **414**, 33 (2001).
[13] H. Chen, T. Ran, Y. Gan, J. Zhou, Y. Zhang, L. Zhang, D. Zhang, and L. Jiang, Ultrafast water harvesting and transport in hierarchical microchannels, Nat. Mater. **17**, 935 (2018).
[14] L. Guo and G. H. Tang, Experimental study on directional motion of a single droplet on cactus spines, Int. J. Heat Mass Transf. **84**, 198 (2015).
[15] J. Ju, H. Bai, Y. Zheng, T. Zhao, R. Fang, and L. Jiang, A multi-structural and multi-functional integrated fog collection system in cactus, Nat. Commun. **3**, 1247 (2012).
[16] C. Luo, Theoretical exploration of barrel-shaped drops on cactus spines, Langmuir **31**, 11809 (2015).
[17] Z. Pan, W. G. Pitt, Y. Zhang, N. Wu, Y. Tao, and T. T. Truscott, The upside-down water collection system of syntrichia caninervis, Nat. Plants **2**, 16076 (2016).
[18] F. T. Malik, R. M. Clement, D. T. Gethin, D. Beysens, R. E. Cohen, W. Krawszik, and A. R. Parker, Dew harvesting efficiency of four species of cacti, Bioinspir. Biomim. **10**, 036005 (2015).
[19] M. E. R. Shanahan, On the behavior of dew drops, Langmuir **27**, 14919 (2011).
[20] X. Tan, T. Shi, Z. Tang, B. Sun, L. Du, Z. Peng, and G. Liao, Investigation of fog collection on cactus-inspired structures, J. Bionic Eng. **13**, 364 (2016).
[21] Y. Chen, L. Wang, Y. Xue, L. Jiang, and Y. Zheng, Bioinspired tilt-angle fabricated structure gradient fibers: Micro-drops fast transport in a long distance, Sci. Rep. **3**, 2927 (2013).
[22] H. Bai, X. Tian, Y. Zheng, J. Ju, Y. Zhao, and L. Jiang, Direction controlled driving of tiny water drops on bioinspired artificial spider silks, Adv. Mater. **22**, 5521 (2010).
[23] M. Cao, J. Ju, K. Li, S. Dou, K. Liu, and L. Jiang, Facile and large-scale fabrication of a cactus-inspired continuous fog collector, Adv. Funct. Mater. **24**, 3235 (2014).
[24] X. Heng, M. Xiang, Z. Lu, and C. Luo, Branched zno wire structures for water collection inspired by cacti, ACS Appl. Mater. Interfaces **6**, 8032 (2014).
[25] Y. Hou, L. Gao, S. Feng, Y. Chen, Y. Xue, L. Jiang, and Y. Zheng, Temperature-triggered directional motion of tiny water droplets on bioinspired fibers in humidity, Chem. Commun. **49**, 5253 (2013).
[26] J. Ju, K. Xiao, X. Yao, H. Bai, and L. Jiang, Bioinspired conical copper wire with gradient wettability for continuous and efficient fog collection, Adv. Mater. **25**, 5937 (2013).
[27] T. Xu, Y. Lin, M. Zhang, W. Shi, and Y. Zheng, High-efficiency fog collector: Water unidirectional transport on heterogeneous rough conical wires, ACS Nano **10**, 10681 (2016).
[28] T.-S. Wong, S. H. Kang, S. K. Y. Tang, E. J. Smythe, B. D. Hatton, A. Grinthal, and J. Aizenberg, Bioinspired self-repairing slippery surfaces with pressure-stable omniphobicity, Nature (London) **477**, 443 (2011).
[29] D. Dowson, *History of Tribology*, 2nd ed. (Wiley, London, 1998).
[30] K. J. Ruschak, Coating flows, Annu. Rev. Fluid Mech. **17**, 65 (1985).
[31] D. Quéré, Fluid coating on a fiber, Annu Rev. Fluid Mech. **31**, 347 (1999).
[32] S. J. Weinstein and K. J. Ruschak, Coating flows, Annu. Rev. Fluid Mech. **36**, 29 (2004).

[33] J. H. Snoeijer, J. Ziegler, B. Andreotti, M. Fermigier, and J. Eggers, Thick Films of Viscous Fluid Coating a Plate Withdrawn from a Liquid Reservoir, Phys. Rev. Lett. **100**, 244502 (2008).
[34] E. Rio and F. Boulogne, Withdrawing a solid from a bath: How much liquid is coated? Adv. Colloid Interface Sci. **247**, 100 (2017).
[35] P.-G. de Gennes, F. Brochart-Wyart, and D. Quéré, *Capillarity and Wetting Phenomena: Drops, Bubbles, Pearls, Waves* (Springer, New York, 2003).
[36] L. D. Landau and B. V. Levich, Dragging of a liquid by a moving plate, Acta Phys.-Chim. USSR **17**, 42 (1942).
[37] B. V. Derjaguin, On the thickness of a layer of liquid remaining on the walls of vessels after their emptying, and the theory of the application of photoemulsion after coating on the cine film, Acta Phys.-Chim. USSR **20**, 349 (1943).
[38] M. Maleki, M. Reyssat, F. Restagno, D. Quéré, and C. Clanet, Landau-Levich menisci, J. Colloid Interface Sci. **354**, 359 (2011).
[39] A. De Ryck and D. Quéré, Inertial coating of a fibre, J. Fluid Mech. **311**, 219 (1996).
[40] A. Q. Shen, B. Gleason, G. H. McKinley, and H. A. Stone, Fiber coating with surfactant solutions, Phys. Fluids **14**, 4055 (2002).
[41] F. P. Bretherton, The motion of long bubbles in tubes, J. Fluid Mech. **10**, 166 (1961).
[42] G. K. Batchelor, *An Introduction to Fluid Dynamics* (Cambridge University Press, Cambridge, 1967).
[43] A. Oron, S. H. Davis, and S. G. Bankoff, Long-scale evolution of thin liquid films, Rev. Mod. Phys. **69**, 931 (1997).
[44] A. Logg, K.-A. Mardal, and G. Wells, *Automated Solution of Differential Equations by the Finite Element Method: The FEniCS Book* (Springer Science & Business Media, Berlin, 2012), Vol. 84.